BOSE-EINSTEIN CONDENSATES STUDIED WITH A LINEAR ACCELERATOR

CH. BUGGLE, J. LEONARD,* W. VON KLITZING,† AND
J. T. M. WALRAVEN

FOM Institute for Atomic and Molecular Physics,
Kruislaan 407, 1098 SJ Amsterdam, The Netherlands
and
Van der Waals-Zeeman Institute of the University of Amsterdam,
Valckenierstraat 65/67, 1018 XE The Netherlands
E-mail: walraven@science.uva.nl

We present a stand-alone interference method for the determination of the s- and d-wave scattering amplitudes in a quantum gas. Colliding two ultracold atomic clouds we observe the halo of scattered atoms in the rest frame of the collisional center of mass by absorption imaging. The clouds are accelerated up to energies at which the scattering pattern shows the interference between the s- ($l = 0$) and d- ($l = 2$) partial waves. With computerized tomography we transform the images to obtain the angular distribution, which is directly proportional to the differential cross section. This allows us to measure the asymptotic phase shifts of the s- and d-wave scattering channels. The method does not require knowledge of the atomic density. It allows us to infer accurate values for the s- and d-wave scattering amplitudes from the zero-energy limit up to the first Ramsauer-Townsend minimum using only the Van der Waals C_6 coefficient as theoretical input. For the ^{87}Rb triplet potential, the method yields an accuracy of 6%.

1. Introduction

The scattering length, the elastic scattering amplitude in the zero-energy limit, is a key parameter in the theoretical description of quantum gases.[1] The scattering length a determines the kinetic properties of these gases as well as the bosonic mean field. Its sign is decisive for the collective stability of the Bose-Einstein condensed state. Near scattering resonances, pairing behavior and three-body lifetime can also be expressed in terms of a. As a consequence, the determination of the low-energy elastic scattering

---

*present address: Université de Strasbourg, Institut de Physique et Chimie des Materiaux.
†present address: IESL - FORTH, Vassilika Vouton, 711 10 Heraklion, Greece.

2

properties is a key issue to be settled prior to further investigation of any new quantum gas.

Over the past decade the crucial importance of the scattering length has stimulated important advances in collisional physics.[2] In all cases except hydrogen the scattering length has to be determined experimentally as accurate *ab initio* calculations are not possible.[3] An estimate of the modulus $|a|$ can be obtained relatively simply by measuring kinetic relaxation times.[4] In some cases the sign of a can be determined by such a method, provided p- or d-wave scattering can be neglected or accounted for theoretically.[5] These methods have a limited accuracy since they rely on the knowledge of the atomic density and kinetic properties. Precision determinations are based on photo-association,[6] vibrational-Raman,[7] and Feshbach-resonance spectroscopy,[8,9] or a combination of those. They require refined knowledge of the molecular structure in ground and excited electronic states.[2]

In this contribution we describe a new method to determine the scattering length by studying the halo of scattered atoms after the collision of two ultracold atomic clouds.[10] We compare our results with related work.[11,12]

2. The accelerator

We start our experiments by loading about one billion ^{87}Rb atoms into a magneto-optical trap (MOT). After optical pumping into the fully stretched $|5^2S_{1/2}, F = 2, m_F = 2\rangle$ hyperfine level, the atoms are transferred into a Ioffe-Pritchard trap (21×477 Hz) with an offset field of $B_0 = +0.9$ G. We pre-cool the atomic cloud to about $6\,\mu$K using forced radio-frequency (RF) evaporation. To prepare for a collision experiment, the cloud is split in two parts by applying a rotating magnetic field and ramping B_0 down to a negative value B_0^-. This results in two Time-averaged Orbiting Potential (TOP) traps loaded with atoms.[13] By RF-evaporative cooling we reach Bose-Einstein condensation with about 10^5 atoms in each cloud and a condensate fraction of $\sim 60\%$.

By switching off the TOP fields and ramping B_0 back to positive values we linearly accelerate the clouds until they collide with opposite horizontal momenta at the location of the trap center. The collision energy $E = |2\mu_B B_0^-| = \hbar^2 k^2/m$ (with μ_B the Bohr magneton and m the mass of ^{87}Rb) can be varied from 138 μK to 1.23 mK with an overall uncertainty of 3% (RMS). Approximately 0.5 ms before the collision we switch off the trap. A few ms later a halo of scattered atoms is observed by absorption imaging (see Fig. 1).
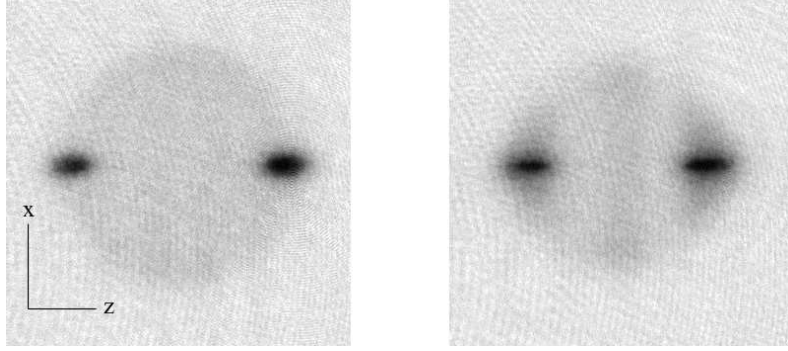
Figure 1.   Left: Scattering halo of two ^{87}Rb condensates for collision energy $E/k_B = 138(4)\,\mu$K (mostly s-wave scattering), measured 2.4 ms after the collision; Right: idem but measured 0.5 ms after a collision at 1230(40) μK (mostly d-wave scattering). The field of view of the images is $\sim 0.7 \times 0.7$mm^2.

3. Data analysis

As the atoms are scattered by a central field, the scattering pattern must be axially symmetric around the (horizontal) scattering axis (z-axis). This allows a computerized tomography transformation to reconstruct the radial density distribution of the halo in cylindrical coordinates,[14]

$$n\left(\rho,z\right) = \frac{1}{4\pi} \int_{-\infty}^{\infty} \tilde{n}_2\left(\kappa_x, z\right) J_0\left(\kappa_x \rho\right) \left|\kappa_x\right| d\kappa_x. \tag{1}$$

Here $\rho = (x^2 + y^2)^{1/2}$ is the radial coordinate and $\tilde{n}_2\left(\kappa_x, z\right)$ the 1D Fourier transform along the x-direction of the optical density with respect to z; $J_0\left(\varrho\right)$ is the zero-order Bessel function.

From the radial density distribution of the halo we obtain the angular scattering distribution, which (for gas clouds much smaller than the diameter of the halo) is directly proportional to the differential cross section

$$\sigma\left(\theta\right) = 2\pi \left|f\left(\theta\right) + f\left(\pi - \theta\right)\right|^2. \tag{2}$$

Here, the Bose-symmetrized scattering amplitude is given by a summation over the even partial waves,

$$f\left(\theta\right) + f\left(\pi - \theta\right) = (2/k) \sum_{l=even} (2l+1) e^{i\eta_l} P_l(\cos\theta) \sin\eta_l. \tag{3}$$

Given the small collision energy in our experiments, only the s- and d-wave scattering amplitudes contribute,

$$f_s\left(\theta\right) + f_s\left(\pi - \theta\right) = (2/k) e^{i\eta_0} \sin\eta_0$$
$$f_d\left(\theta\right) + f_d\left(\pi - \theta\right) = (2/k)(5/2) e^{i\eta_2} \left(3\cos^2\theta - 1\right) \sin\eta_2.$$

4

Therefore, the differential cross section is given by a quadratic expression,

$$\sigma(\theta) = \frac{8\pi}{k^2} \sin^2 \eta_0 \left[1 + 5\cos(\eta_0 - \eta_2)u + \frac{25}{4}u^2 \right], \qquad (4)$$

with $u \equiv (\sin \eta_2 / \sin \eta_0) \left(3\cos^2 \theta - 1 \right)$.

As suggested by Eq. (4), we make a parabolic fit to the measured angular distribution plotted as a function of $\left(3\cos^2 \theta - 1 \right)$. This yields directly a pair of asymptotic phase shifts $[\eta_0^{\mathrm{exp}}(k), \eta_2^{\mathrm{exp}}(k)]$ - defined modulo π - corresponding to the two partial waves involved.[15] The absolute value of $\sigma(\theta)$ depends on quantities that are hard to measure accurately (like the atom number) so we leave it out of consideration. We rather emphasize that the measurement of the phase shifts allows a *complete* determination of the (complex) s- and d-wave scattering amplitudes at a given energy.

4. Determination of the energy dependence

The radial wavefunctions corresponding to scattering at different (low) collision energies and different (low) angular momenta should all be in phase at small interatomic distances.[16] This so-called *accumulated phase* is common to all low-energy wave functions and is extracted by a least-square fit to the full data set $\{\eta_0^{\mathrm{exp}}(k), \eta_2^{\mathrm{exp}}(k)\}$. In practice, we use the experimental phase shifts $\eta_0^{\mathrm{exp}}(k)$ and $\eta_2^{\mathrm{exp}}(k)$ as boundary conditions to integrate inwards the Schrödinger equation $\hbar^2 d^2\chi(r)/dr^2 + p^2(r)\chi(r) = 0$ for given E and l, and obtain the radial wavefunctions $\chi(r)/r$ down to radius $r_{in} = 20\,a_0$. Here, $p^2(r) = m\left(E - V(r)\right) - \hbar^2 l(l+1)/r^2$, where $V(r) \simeq -C_6/r^6$ approximates the tail of the interaction potential. At radius $20\,a_0$, the motion of the atoms is quasi-classical and the accumulated phase can be written as $\Phi(r) \simeq \arctan\left[p(r)/(\hbar\,\partial \ln \chi/\partial r)\right]$. The distance $20\,a_0$ is small enough for $\Phi(r_{in})$ to be highly insensitive to small variations in E or l but also large enough for the $-C_6/r^6$ part of the interaction potential to be dominant over the full range of integration.[16] With a least-square procedure we establish the best value $\Phi_{\mathrm{opt}}(r_{in}) = 1.34 \pm (\pi \times 0.025)$ for the accumulated phase at $20\,a_0$. Here the error bar reflects the experimental accuracy and not the systematic error related to the choice of C_6. The d-wave scattering resonance results in a sudden variation of η_2^{exp} with the collision energy in the vicinity of that resonance (see Fig. 2a).[17] This imposes a stringent condition on the optimization of Φ_{opt} and constrains its uncertainty.

We emphasize that Φ_{opt} has no physical significance but is valuable as a boundary condition to integrate the Schrödinger equation back outwards to compute $\eta_l(k)$ for any desired (low) value of k and l. Fig. 2 shows the
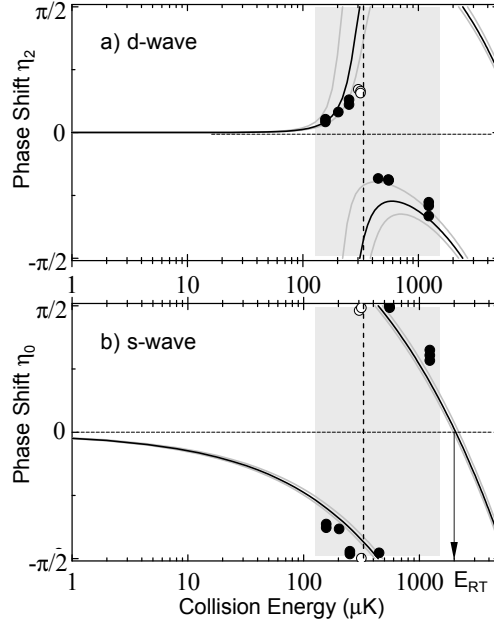
Figure 2.   a) d-wave and b) s-wave phase shifts versus collision energy in μK; s-d interference is only observed in the gray areas. The circles are the results of the parabolic fits for individual images. The full black lines is calculated from the accumulated phase Φ_{opt} optimized from all data points. The grey lines show the influence of the uncertainty of $\pm(\pi \times 0.025)$ on Φ_{opt}. The vertical dotted line indicates the condition $\eta_0 = \eta_2$. The first s-wave Ramsauer-Townsend minimum is found at $E_{RT} = 2.1(2)$ mK.

resulting phase shifts for collision energies up to 5 mK. The first Ramsauer-Townsend minimum in the s-wave cross section is found at collision energy $E_{RT}/k_B = 2.1(2)$ mK. The solid dots represent the $\eta_l^{\mathrm{exp}}(k_i)$ obtained from the parabolic fits for individual images. The three open circles correspond to measurements for which the sign of the phase shifts could not be established.[10] Refinements to the procedure may account for multiple scattering effects as well as the presence of a non condensed fraction.

Note that this procedure does not require knowledge of the density of the clouds, unlike the stimulated raman detection scheme.[18] Knowing the phase shifts, we can infer all low-energy scattering properties. In particular, the total elastic scattering cross section is given by

$$\sigma = \int_0^{\pi/2} \sigma(\theta) \sin\theta d\theta = (8\pi/k^2) \sum_{l=even} (2l+1) \sin^2 \eta_l. \qquad (5)$$
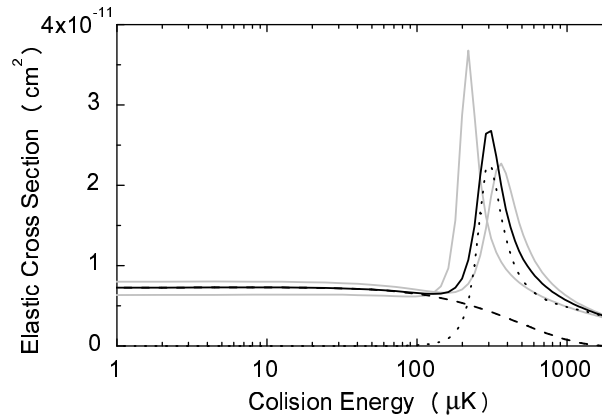
6

Figure 3.   s-wave (dashed line), d-wave (dotted line) and total (full black line) elastic cross sections (in cm^2) versus collision energy (in μK), computed from the optimized accumulated phase Φ_{opt} as determined in this work. The gray lines are the total elastic cross sections, obtained from $\Phi_{opt} \pm (\pi \times 0.025)$.

Note that the total cross section, unlike the differential cross section, does not contain interference terms. Our results are shown in Fig. 3. The (asymmetric) d-wave resonance emerges pronouncedly at 300(70) μK with an approximate width of 150 μK (FWHM). Most importantly, the scattering length follows from the $k \to 0$ limiting behavior, $\eta_0(k \to 0) = -ka$. We find $a = +102(6)\, a_0$, whereas the state-of-the-art value is $a = 98.99(2)\, a_0$.[19]

5. Comparison with related work

Comparison of our results with the precision determinations shows that our method is fairly accurate, although it only relies on the input of the C_6 coefficient. We used the value $C_6 = 4.698(4) \times 10^3$ a.u..[19] In the present case, one does not need to know C_6 to this accuracy. Increasing C_6 by 10% results in a 1 %-change of our computed scattering length. Clearly, the systematic error in Φ_{opt} accumulated by integrating the Schrödinger equation inward with a wrong C_6 largely cancels when integrating back outward. However, in the case of a s-wave resonance other atomic species may reveal a stronger influence of C_6 on the calculated scattering length. Simple numerical simulations show that the value of C_6 becomes critical only when the (virtual) least-bound state in the interaction potential has an extremely small (virtual) binding energy (less than 10^{-2} level spacing). Hence our method should remain accurate in almost any case.

We point out that our method do not require the use of Bose-Einstein condensed ultracold clouds. However, the use of condensates is practical as they allow high energy resolution and analysis of the largest possible window of scattering angles. At the University of Otago similar collision experiments were done with *thermal* clouds of ^{87}Rb in the $|5^2S_{1/2}, F = 2, m_F = 2\rangle$ state.[11] In these experiments the differential and total cross section were measured directly and found to be in good agreement with theory. At this ICOLS conference the Otago/Nist team reported interferometric observation of *p*-wave scattering between *non-identical* bosons by colliding a cloud of ^{87}Rb atoms in the $|5^2S_{1/2}, F = 1, m_F = -1\rangle$ state with a ^{87}Rb cloud in the $|5^2S_{1/2}, F = 2, m_F = 1\rangle$ state.[20]

We finally point to the relation between the halos observed in our experiments and those observed by dissociation of ^{87}Rb-dimers near a Feshbach resonance at the Max Planck Institute for Quantum Optics (MPQ) in Garching.[12] In these experiments interference was observed between dissociation halos from the *s*- and *d*-wave channels by Feshbach tuning the dissociation energy to the value corresponding to the *d*-wave resonance. Like in our experiments the final state pair wave functions can be written in the dissociation case as

$$\Psi(\mathbf{r}, t) = g(r, t) \left[e^{i\eta_0} \sqrt{\beta_0} Y_0^0 + e^{i\eta_2} \sqrt{\beta_2} Y_2^0(\theta) \right], \tag{6}$$

where β_0 and β_2 (with $\beta_0 + \beta_2 = 1$) are the branching ratios for the *s*- and *d*-wave channels, respectively and η_0 and η_2 set their relative asymptotic phase. For the collision experiments the branching ratios depend on the phase shifts η_0 and η_2 and on the decomposition of the incident plane waves into partial waves, and are given by

$$\beta_0 = \frac{\sin^2 \eta_0(k)}{\sin^2 \eta_0(k) + 5 \sin^2 \eta_2(k)} \text{ and } \beta_2 = 1 - \beta_0. \tag{7}$$

In the dissociation experiments there is no incident wave, but the phase difference $\eta_2 - \eta_0$ remains well defined and agrees with our experiments. Therefore, the difference between the two experimental situations shows up as a difference in branching ratios.

Acknowledgments

8

References

1. See *e.g.* L. Pitaevskii and S. Stringari, *Bose-Einstein condensation*, Clarendon Press, Oxford 2003; C.J. Pethick and H. Smith, *Bose-Einstein condensation in dilute gases*, Cambridge University Press, Cambridge 2002.
2. J. Weiner, V.S. Bagnato, S. Zilio, P.S. Julienne, *Rev. Mod. Phys.* **71**,1 (1999).
3. D.G. Friend and R.D. Etters, *J. Low Temp. Phys.* **39**, 409 (1980); Y.H. Uang and W.C. Stwalley, *J. de Phys.* 41, C7-33 (1980).
4. C. R. Monroe *et al.*, *Phys. Rev. Lett.* **70**, 414 (1993); S. D. Gensemer *et al.*, *Phys. Rev. Lett.*, **87**, 173201 (2001).
5. G. Ferrari *et al.*, *Phys. Rev. Lett.* **89**, 53202 (2002); P. Schmidt *et al.*, *Phys. Rev. Lett.* **91**, 193201 (2003).
6. D. Heinzen in: *Proceedings of the international School of Physics, Enrico Fermi*, M. Inguscio, S. Stringari and C. Wieman (Eds.), IOS Press, Amsterdam 1999.
7. C. Samuelis, E. Tiesinga, T. Laue, M. Elbs, H. Knckel and E. Tiemann, *Phys. Rev. A* **63**, 12710 (2001).
8. C. Chin, V. Vuletic, A. J. Kerman, and S. Chu, *Phys. Rev. Lett.* **85**, 2717 (2000); P. J. Leo, C. J. Williams, and P. S. Julienne, *Phys. Rev. Lett.* **85**, 2721 (2002).
9. A. Marte, T. Volz, J. Schuster, S. Drr, G. Rempe, E. G. M. van Kempen, and B. J. Verhaar, *Phys. Rev. Lett.* **89**, 283202 (2002).
10. Ch. Buggle, J. Leonard, W. von Klitzing and J.T.M. Walraven, *Phys. Rev. Lett.* **93** 173202 (2004)
11. N.R. Thomas, N. Kjærgaard, P.S. Julienne, and A.C. Wilson, *Phys. Rev. Lett.* **93** 173201 (2004).
12. T. Voltz, S.Durr, N. Syassen, G. Rempe, E. van Kempen, S. Kokkelmans, cond-mat/0410083.
13. T.G. Tiecke, M. Kemmann, Ch. Buggle, I. Schvarchuck, W. von Klitzing and J.T.M. Walraven, *J. Opt. B* **5**, S119 (2003); see also N. R. Thomas, A. C. Wilson, and C. J. Foot, *Phys. Rev. A* **65**, 063406 (2002).
14. M. Born and E. Wolf, *Principles of Optics*, 7th (expanded) Edition, Cambridge University Press, Cambridge 1999.
15. This procedure breaks down in the marginal case $\eta_0 = \eta_2$, where the expression in the square brackets in Eq. (4) becomes phase-shift independent.
16. B. Verhaar, K. Gibble, and S. Chu, *Phys. Rev. A* **48**, R3429 (1993); G.F. Gribakin and V.V. Flambaum, *Phys. Rev. A* **48**, 546 (1993).
17. H.M.J.M. Boesten, C.C. Tsai, J.R. Gardner, D. J. Heinzen, B.J. Verhaar, *Phys. Rev. A* **55**, 636 (1997).
18. R. Legere and K. Gibble, *Phys. Rev. Lett.* **81**, 5780 (1998).
19. E.G.M. van Kempen, S.J.J.M.F. Kokkelmans, D.J. Heinzen, and B.J. Verhaar, *Phys. Rev. Lett.* **88**, 93201 (2002).
20. A.S. Mellish, N. Kjærgaard, A.C. Wilson and P.S. Julienne, This meeting, Poster 97.